Lipid bilayers decorated with photosensitive ruthenium complexes

Bahreman, A.

4

Binding of a ruthenium complex to a thioether ligand embedded in a negatively charged lipid bilayer:

a two-step mechanism

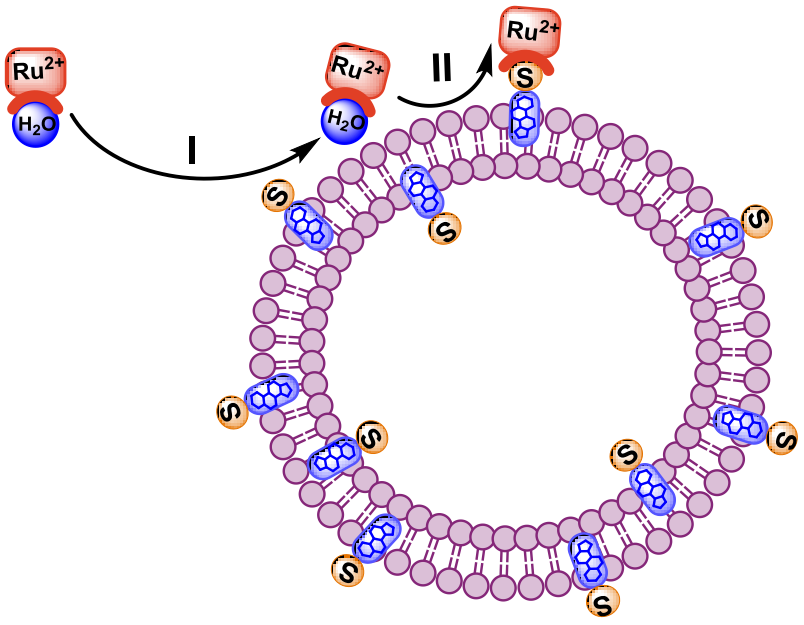

This Chapter has been submitted as a paper;
Bahreman A.; Rabe M.; Kros A.; Bruylants G.; Bonnet S.; *submitted for publication.*

Abstract

The interactions between the ruthenium polypyridyl complex $[Ru(terpy)(dcbpy)(H_2O)]^{2+}$ (terpy=2,2';6',2"-terpyridine, dcbpy=6,6'-dichloro-2,2'-bipyridine) and phospholipid membranes containing either neutral thioether ligands or cholesterol were investigated using UV-visible spectroscopy, Langmuir-Blodgett monolayer surface pressure measurements, and Isothermal Titration Calorimety (ITC). The first technique shows that when embedded in a membrane a thioether ligand coordinates to the ruthenium complex only with negatively charged phospholipids, *i.e.,* in presence of attractive electrostatic interaction between the dicationic ruthenium center and the negatively charged phospholipid head groups. Lipid monolayer surface pressure and ITC measurements revealed that initial adsorption of the ruthenium aqua complex to the surface of negatively charged DMPG monolayers and bilayers is faster than coordination of the sulfur ligand to the metal. Unexpectedly this adsorption phenomenon is endothermic, thus entropy driven, and must result from dehydration of the ruthenium cations and phospholipid head groups. In the presence of thioether ligands, initial adsorption to the membrane is followed by two-dimensional diffusion ultimately leading to the formation of the Ru-S coordination bond. This two-step reaction is faster than the coordination of neutral thioether ligands to the same complex in homogeneous aqueous solutions. When an uncharged lipid bilayer is used, adsorption of the complex to the membrane is negligible and the coordination reaction does not occur.

4.1. Introduction

Transition metal complexes, and in particular those involving second- and third-row metals like platinum, ruthenium, or gold, have been extensively studied as anticancer agents.[1] To explain their cytotoxicity, direct coordination of the metal complexes to the binding sites of biomolecules such as DNA[2-3] or proteins[4] has been proposed. Next to coordination, non-covalent interactions such as electrostatic force or/and intercalation may also play a role.[5] However, interpreting the mode of action of metallodrugs is often considered to be a challenge,[6] as cellular environments contain a striking diversity of ligands that may bind to metal complexes, such as proteins, enzymes, saccharides, or plasma membrane lipids. On the one hand, interactions of metallodrugs with non-targeted ligands may be the cause of drug resistance or non-selective toxicity. Phospholipids, in particular, have been reported as possible targets for platinum-based drugs,[7] whereas membrane proteins, which are formally ligands embedded in lipid bilayers, often govern influxes and effluxes of metal-based anticancer compounds. [4, 8-9] On the other hand, the metal-lipid affinity may be used as a tool to carry metallodrugs to its target using liposomes.[10-12] In this context, investigating the interactions of metal complexes with phospholipids or ligands embedded in lipid bilayers is crucial for understanding and controlling the therapeutic action of inorganic compounds.

The electrostatic interaction between phospholipids and metal cations, in particular alkali or alkaline earth metals like Na^+ and Ca^{2+}, have been extensively investigated.[13-25] However, to date very few studies report on the interaction of transition metal complexes with phospholipid membranes.[7, 26-32] Despite the growing number of ruthenium-based anticancer compounds their interaction with phospholipid membranes remains essentially unexplored, with the exception of a study on the adsorption of the highly charged ruthenium red cations on phospholipid bilayers.[33] In all published studies, the role of electrostatic interaction between metal cations and negative phospholipids is only investigated from a thermodynamic point of view, and kinetics has been mostly ignored.

On our way to building artificial molecular machines based on polypyridyl ruthenium complexes[34] the reversible binding and light-induced unbinding of the ruthenium aqua complex $[Ru(terpy)(dcbpy)(H_2O)]^{2+}$ (terpy:2,2';6',2"-terpyridine, dcbpy: 6,6'-dichloro-2,2'-bipyridine) to thioether ligands embedded in negatively charged phospholipid

bilayers was demonstrated in Chapter 2 (Figure 4.1). In these studies, it was observed that whereas coordination of neutral thioether ligands to ruthenium aqua complexes occurred in homogenous aqueous solution, incorporating the thioether ligand in a lipid bilayer had strong influence on the coordination reaction, which becomes highly dependent on the charge of the membrane. Centrifugation experiments showed that positively charged ruthenium aqua complexes interact significantly with negatively charged lipid bilayers, irrespective whether or not the thioether-cholesterol ligand was present.[34]

In the present Chapter UV-vis spectroscopy, Langmuir-Blodgett monolayer surface pressure measurements, and calorimetric methods were used to investigate the time scale and thermodynamics of the adsorption of the ruthenium complex to the lipid membranes, and to see whether adsorption and coordination of the membrane-embedded ligands to the metal occur simultaneously or sequentially. A two-step mechanism for the binding of ruthenium complexes to membrane-embedded thioether ligands is proposed.

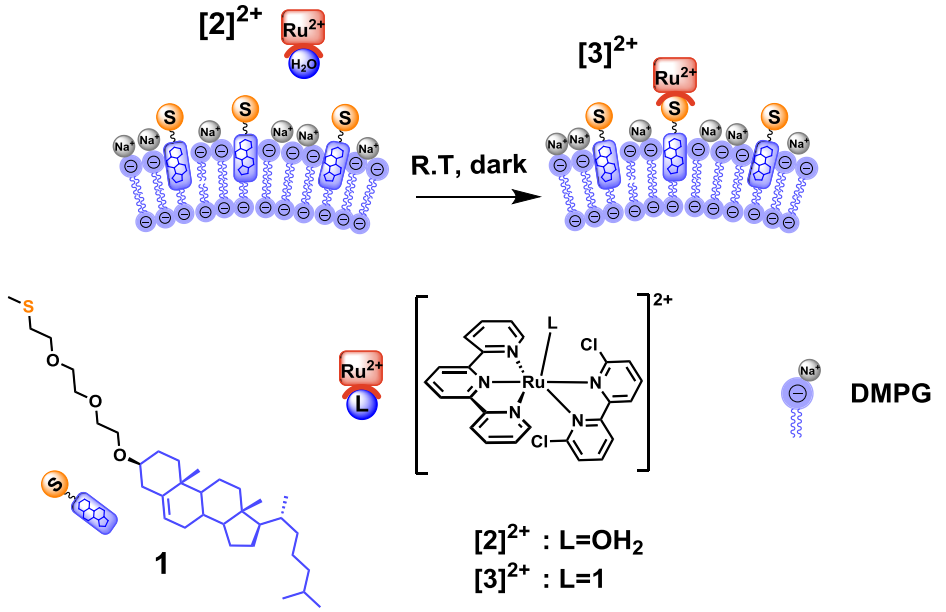

Figure 4.1. Cartoon representing the thermal binding of the ruthenium aqua complex $[\mathbf{2}]^{2+}$ to a DMPG (1,2-dimyristoyl-*sn*-glycero-3-phospho-(1'-rac-glycerol) (sodium salt)) lipid bilayer containing ligand **1**, to give the thioether complex $[\mathbf{3}]^{2+}$. Not all sodium cations are shown for clarity.

4.2. Results

4.2.1. UV-vis experiments

UV-vis experiments were performed in order to check the influence of the electrostatic interaction between liposomes and ruthenium complexes on the rate of the coordination reaction at the membrane surface. The kinetics of the coordination of thioether-cholesterol ligand **1** inserted in negatively charged DMPG (DMPG=1,2-dimyristoyl-*sn*-glycero-3-phospho-(1'-rac-glycerol) sodium salt) liposomes to the ruthenium complex $[Ru(terpy)(dcbpy)(H_2O)]^{2+}$ (compound $[\mathbf{2}]^{2+}$) was investigated in buffer solutions with different ionic strengths at 298 K and in the dark (Figure 4.1). Liposomes decorated with 25 mol% ligand **1** with diameter of 140 nm were prepared as characterized by dynamic light scattering (DLS). After addition of 5 mol% of the aqua ruthenium complex $[\mathbf{2}]^{2+}$ the UV-vis spectrum of the liposome solution gradually evolved and an equilibrium was obtained after several hours. The liposomes were stable during the reaction and did not show any sign of aggregation or fusion at the end of the reaction as confirmed by DLS. The absorbance at 500 nm decreased exponentially over time (see Figure 4.2b-I, for I=50 mM), which allowed for determining the half reaction time ($t_{1/2}$) for the coordination reaction. The plot of $t_{1/2}$ *vs.* the ionic strength I of the buffer solution is shown in Figure 4.2a. As expected, the half-reaction time increased almost linearly with *I, i e.*, the ligand substitution became slower when the electrostatic interaction between the ruthenium dications and the negative liposomes was shielded by the other ions present in solution. Interestingly, the coordination reaction at the surface of negatively charged membranes is significantly faster than that in homogenous aqueous solution using thioether ligands not bound to liposomes. The kinetics for the coordination of the water-soluble thioether ligand 2-(methylthio)ethanol (Hmte) to $[\mathbf{2}]^{2+}$ was already reported in Chapter 2 and follows a second-order rate law with a second-order rate constant 2.3×10^{-2} $M^{-1}\cdot s^{-1}$ at 297 K. However, with the low concentration used (*i.e.*, 0.3 mM for Hmte and 0.067 mM for $[\mathbf{2}]^{2+}$) the coordination rate in a I=50 mM buffer solution is very low as $t_{1/2}$ is over 68 h (Figure 4.2a-IV) while the coordination at DMPG membranes showed to have $t_{1/2}$~2.6 h (see Figure 4.2a-I).

To prove that the charge of the liposome is the major factor controlling the kinetics of the coordination, two control experiments were performed. In the first experiment, the coordination reaction was performed using another negatively charged lipid 1,2-

dioleoyl-*sn*-glycero-3-phospho-(1'-rac-glycerol) sodium salt (hereafter DOPG)). DOPG liposomes containing 25 mol% ligand **1** were mixed with 5 mol% $[\mathbf{2}]^{2+}$ in the dark. As shown in Figure 4.2b-II, the kinetics of the reaction with DOPG is almost the same as that with DMPG liposomes, in a buffer with I=50 mM ($t_{1/2}$ =154 min and 160 min, respectively). Thus, the kinetics of the reaction are almost the same for two different negatively charged liposomes. A second control experiment was performed with non-charged liposomes to check the influence of hydrophobic interactions. Neutral liposomes made of DOPC (DOPC=1,2-dioleoyl-*sn*-glycero-3-phosphocholine) and functionalized with the same amount of ligand **1** (25 mol%) were prepared. After addition of $[\mathbf{2}]^{2+}$ the UV-vis spectrum of the solution remained unchanged at least for 20 hours in the dark, which is longer than the longest experiment (I~1000 mM) realized with DMPG liposomes (Figure 4.2b-III). Overall, These experiments confirm that the electrostatic interaction between the ruthenium complex and the surface of the lipid bilayer is crucial for the binding of the Ru(II) cations to the sulfur atom of ligand **1** embedded in a lipid bilayer.

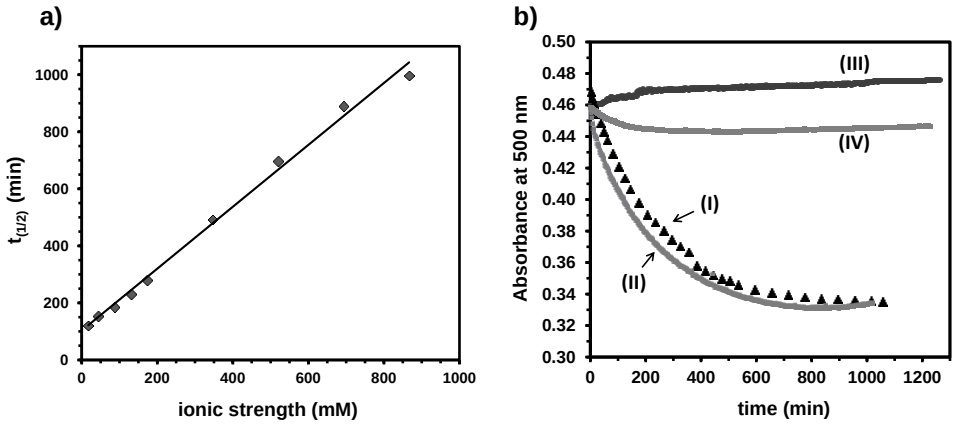

Figure 4.2. a) Plot of the half reaction time $t_{1/2}$ *vs.* the total ionic strength I of the buffer for the thermal binding of aqua complex $[\mathbf{2}](PF_6)_2$ to ligand **1** incorporated in DMPG liposomes. b) Time evolution of the absorbance at 500 nm for a solution containing (I) DMPG, (II) DOPG, (III) DOPC liposomes containing 25 mol% of ligand **1**, or (IV) Hmte (no liposome), after addition of $[\mathbf{2}](PF_6)_2$ at t=0, using a 10 mM phosphate buffer at pH=7 with a total ionic strength of 50 mM. Conditions for a) and b): in the dark, T = 298 K, total concentration of $[\mathbf{2}]^{2+}$=0.067 mM, bulk concentration of ligand **1** or Hmte=0.3 mM in all samples, lipid concentration= 1.3 mM (as liposomes in plot b-IV lipid concentration is 0 mM).

In all these experiments however, UV-vis spectroscopy could only probe changes occurring in the coordination sphere of the metal center. It does not allow for studying changes in the environment of the complex that would not involve ligand exchange, such as for example the adsorption of the ruthenium aqua complex at the water-bilayer interface. Two other experimental techniques, *i.e*, surface pressure measurements on lipid monolayers, and Isothermal Titration Calorimetry (ITC) were used to gain insight into the adsorption step.

4.2.2. Langmiur-Blodgett monolayer experiments

Langmuir monolayers are composed of amphiphilic molecules self-assembled at the air/water interface. The interaction of these monolayers with molecules dissolved in the aqueous subphase can be probed by measuring changes of the surface pressure ($\Delta\Pi$) of the monolayer by means of a platinum Wilhelmy plate. Langmuir monolayers are recognized as a good model for one leaflet of a lipid bilayer,[35] surface pressure measurements were performed to study the interaction of the ruthenium complex $[\mathbf{2}]^{2+}$ with negatively charged and zwitterionic lipid monolayers at the buffer/lipid interphase. First, four types of lipid monolayers were prepared at the air/buffer interface using DMPG, DMPG containing 25 mol% of ligand **1**, DMPC, and DMPC containing 25 mol% of ligand **1** lipid mixtures. Stock solutions of the lipids were spread onto the phosphate buffer subphase (I=50 mM, pH=7, T=298 K) and the monolayer was compressed at a constant rate. Upon compression, the surface pressure (Π) was measured as a function of the area of water surface available to each lipid molecule (A). The surface pressure-area (Π-A) isotherms that were obtained for each sample (see Appendix IV, Figure AIV.1); were in good agreement with previously reported data for DMPG and DMPC monolayers.[36-38] Addition of the thioether-cholesterol ligand **1** to the lipid compositions shifted the Π-A isotherms to lower molecular areas compared to pure DMPG or DMPC, which indicates to a slightly better packing of the monolayer at the air-buffer subphase in presence of **1**.

In a second series of experiments, lipid monolayers of DMPG containing 25 mol% of ligand **1** were prepared on the phosphate subphase at a constant surface pressure, at 298 K and in the dark. After equilibration a buffered solution of $[\mathbf{2}]^{2+}$ was injected into the subphase underneath the lipid film, and the resulting change in surface pressure was recorded as a function of time in the dark. As shown in Figure 4.3a-II after injection of

$[\mathbf{2}]^{2+}$ an increase in the surface pressure takes place within 6-7 min, to reach an equilibrium at a slightly higher pressure. The observed evolution time scale is too short for ligand coordination to the ruthenium complex to be completed (see Figure 4.2b-I). Furthermore, a control experiment was performed using cholesterol as additive instead of ligand **1**. For such sulfur-deprived DMPG monolayers the surface pressure also increased within a couple of minutes after injection of $[\mathbf{2}]^{2+}$, and $\Delta\Pi$ was roughly identical to that observed for the DMPG sample containing ligand **1** (Figure 4.3a-I). Thus, the observed increase of Π cannot be caused by sulfur coordination to the metal.

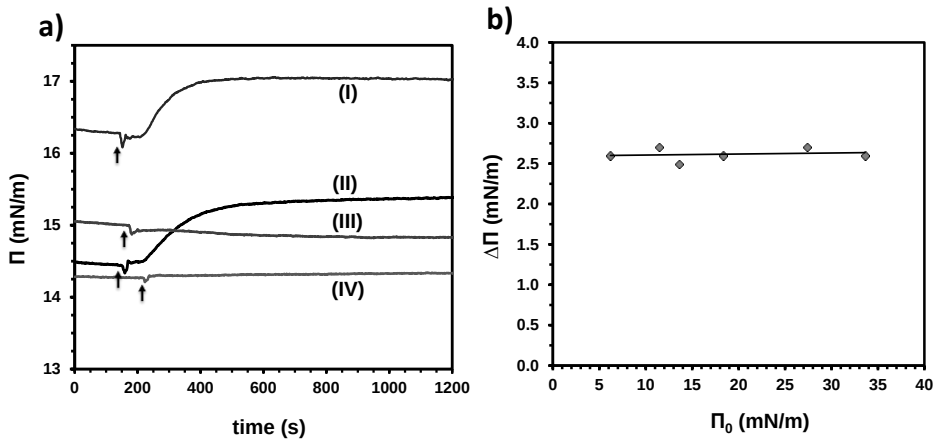

Figure 4.3. a)Plots of surface pressure *vs.* time for phospholipid monolayers after injection of $[\mathbf{2}]^{2+}$ (final concentration= 0.5 µM) into a buffer subphase. (I) DMPG and 25 mol % cholesterol (I=50 mM), (II) DMPG and 25 mol% ligand **1** (I=50 mM), (III) DMPG and 25 mol% ligand **1** (I=400 mM), (IV) DMPC and 25 mol% ligand **1** (I=50 mM). Each arrow represents an injection of 50 µL of $[\mathbf{2}]^{2+}$, Conditions: concentration of $[\mathbf{2}]^{2+}$ in the stock solution = 0.65 mM, T=298 K, pH=7.0, volume of the trough: 65 mL. b) Plot of the surface pressure variation $\Delta\Pi$ as a function of the initial surface pressure Π_0 for data obtained for DMPG monolayers containing 25 mol% ligand **1** after injection of $[\mathbf{2}]^{2+}$ (final concentration=3.5 µM) in a buffer subphase at different initial surface pressure Π_0. Condition: 10 mM phosphate buffer, total ionic strength=50 mM, concentration of $[\mathbf{2}]^{2+}$ in the stock solution=2.3 mM, T=298 K.

Consecutive injection of $[\mathbf{2}]^{2+}$ to the buffer subphase of DMPG monolayers containing either cholesterol or ligand **1** (Π_0=14 mN/m) showed a total surface pressure variation ($\Delta\Pi$) of about 6 mN/m at saturation condition (see Figure AIV.2). Such a surface pressure variation $\Delta\Pi$ was small compared to those reported for penetrating peptides, enzymes, or other lipophilic macromolecules interacting with lipid monolayers, where $\Delta\Pi$ is usually higher than 10 mN/m.[39-45] This qualitative comparison suggested that

insertion of the metal complex into the membrane was limited. Such a conclusion was confirmed by another experiment showing that the surface pressure variation $\Delta\Pi$ was independent of the initial surface pressure of the monolayer, Π_0. When DMPG monolayers containing 25 mol% of ligand **1** at various initial surface pressures were prepared, in all cases injection of $[\mathbf{2}]^{2+}$ (final concentration:3.5 µM) to the subphase led to equal surface pressure increase ($\Delta\Pi$=2.6 mN/m, see Figure AIV.4). As shown in Figure 4.3b, the slope of the plot of $\Delta\Pi$ *vs.* Π_0 is almost zero, which is differs from the behavior of hydrophobic macromolecules that penetrate the hydrophobic core of the monolayer. In such cases, $\Delta\Pi$ typically decreases when the initial surface pressure Π_0 becomes higher,[39-40, 46-48] In fact, the affinity of $[\mathbf{2}]^{2+}$ for the DMPG monolayer is not high. It can be assumed that the ruthenium complex does not penetrate into the lipid monolayer, but rather migrates at the monolayer-water interface and adsorbs to the polar head groups of the phospholipids.[24, 48-49]

In order to investigate whether the incidence of the adsorption process is due to electrostatic or hydrophobic interactions, two control experiments were performed. In the first experiment, a DMPG monolayer containing ligand **1** was formed onto a buffer subphase with a high ionic strength (I=400 mM instead of 50 mM). As shown in Figure 4.3a-III, injections of $[\mathbf{2}]^{2+}$ in the subphase did not affect the surface pressure of the monolayer. Thus, adsorption of the positively charged ruthenium complex at the surface of the DMPG monolayer does not occur when the ionic strength of the subphase is high, which is in good agreement with the UV-vis data and highlights the role played by electrostatic interaction in the adsorption process. The second control consisted in replacing the DMPG lipid by the zwitterionic analogue DMPC. In presence of 25 mol% of ligand **1** in a DMPC monolayer no measurable variation of the surface pressure was observed after injection of complex $[\mathbf{2}]^{2+}$ (Figure 4.3a-IV), which proves the low affinity of the ruthenium complex for the zwitterionic monolayer surface. In addition, it confirms the low hydrophobicity of the ruthenium complex $[\mathbf{2}]^{2+}$ that does not penetrate into the membrane. Overall, our data support the hypothesis that electrostatic forces are crucial for the adsorption of the ruthenium complex at negatively charged membranes and that hydrophobic force does not play a significant role.

4.2.3. ITC experiments

Surface pressure experiments allow for studying the initial adsorption of ruthenium complexes to negatively charged monolayers before the coordination occurs. Considering the fast kinetics of the adsorption process on monolayers ITC measurements were used to determine the thermodynamic parameters characterizing the adsorption of complex $[\mathbf{2}]^{2+}$ at the surface of the lipid bilayers. Titrations of DMPG liposomes supplemented with 25 mol% cholesterol or ligand **1** by a 0.62 mM solution of complex $[\mathbf{2}]^{2+}$ were performed at 298 K, pH=7, and *I*=50 mM. After each ruthenium addition, the return to equilibrium took less than 100s, which confirms that the adsorption step is characterized by fast kinetics, in accordance with the results obtained for the monolayer experiments. As mentioned above, such time scales are significantly shorter than that of the coordination of ligand **1** to complex $[\mathbf{2}]^{2+}$ at the DMPG membrane. In addition the adsorption phenomenon observed by titration of DMPG liposomes containing ligand **1** was found to be endothermic (Figure 4.4-II). For DMPG membranes containing cholesterol an exothermic process was observed during the initial injections of $[\mathbf{2}]^{2+}$, but further addition of $[\mathbf{2}]^{2+}$ led only to an endothermic process similar to that observed with ligand **1** (Figure 4.4-I). The initial exothermic evolution may be related to structural changes in the negatively charged lipid bilayer due to the interaction of a small amount of divalent cations with the cholesterol and/or the DMPG lipids, as reported for Ca^{2+}.[16, 50]

Two control titrations with $[\mathbf{2}]^{2+}$ were made, on the one hand for DMPG liposomes containing 25 mol% cholesterol in presence of a high ionic strength buffer (*I*=400 mM), and on the other hand of zwitterionic DOPC liposomes containing 25 mol% cholesterol using a buffer with *I*=50 mM. The measured heat exchange was negligible in high ionic strength buffer (see plots III and II in Figure 4.4b), and in the case of the DOPC liposomes the heat exchange was even comparable with the heat exchange observed in absence of liposomes. Overall, the results of the ITC measurements are in good agreement with those obtained with UV-vis and surface pressure monolayer experiments. They confirm that adsorption of the ruthenium complexes to negatively charged membranes is a fast process that does not involve coordination to sulfur.

Table 4.1. Thermodynamic data for the adsorption of [**2**]Cl_2 to DMPG liposomes. Conditions: buffer with *I*=50 mM, pH=7 and 298 K, Concentrations: *[lipid]*=2.5 mM, [**2**]Cl_2 in titrating solution:5 mM.

Bilayer additive	**Apparent K_a** (M^{-1})	***ΔH°*** ($kJ \cdot mol^{-1}$)	***ΔG°*** ($kJ \cdot mol^{-1}$)	***ΔS°*** ($kJ \cdot mol^{-1} \cdot K^{-1}$)	**binding stoichiometry (Ru/lipid ratio) n**
Ligand **1** (25 mol%)	$1.8(3)\times10^{+4}$	+9.1 ±0.3	−24	+112	0.28±0.01
cholesterol (25 mol%)	$9.2(10)\times10^{+3}$	+24±1	−23	+160	0.19 ±0.01

Due to the low solubility of [**2**]$(PF_6)_2$ in the buffer saturation of the DMPG liposomes with ruthenium cations could not be reached (Figure 4.4-II). As a consequence, the fit of the model to the experimental data did not give reliable binding parameters. Thus, the counter ions of $[\mathbf{2}]^{2+}$ were changed to chlorides, which allowed to reach much higher ruthenium concentrations (5 mM) and thus for obtaining quantitative information on the thermodynamics of the adsorption process. By dissolving [Ru(tpy)(dcbpy)(Cl)]Cl in an aqueous solution, the coordinated chloride ligand is quickly substituted by an aqua ligand to form [**2**]Cl_2 quantitatively (see Chapter 2 and 3). Changing the counter ions from PF_6^- to Cl^- had a negligible influence on monolayer experiments and ITC data at low ruthenium concentrations (0.62 mM, see Appendix AIV, Figure AIV.5 and Table AIV.1). Titrations of DMPG liposomes containing ligand 25 mol% ligand **1** or cholesterol were undertaken with more concentrated (5 mM) solutions of $[\mathbf{2}]^{2+}$ and more concentrated liposome solutions (lipid concentration: 2.5 mM). Sigmoidal binding curves were obtained, showing that in such conditions saturation of the membrane with ruthenium cations could be reached (Figure 4.4-V and II).

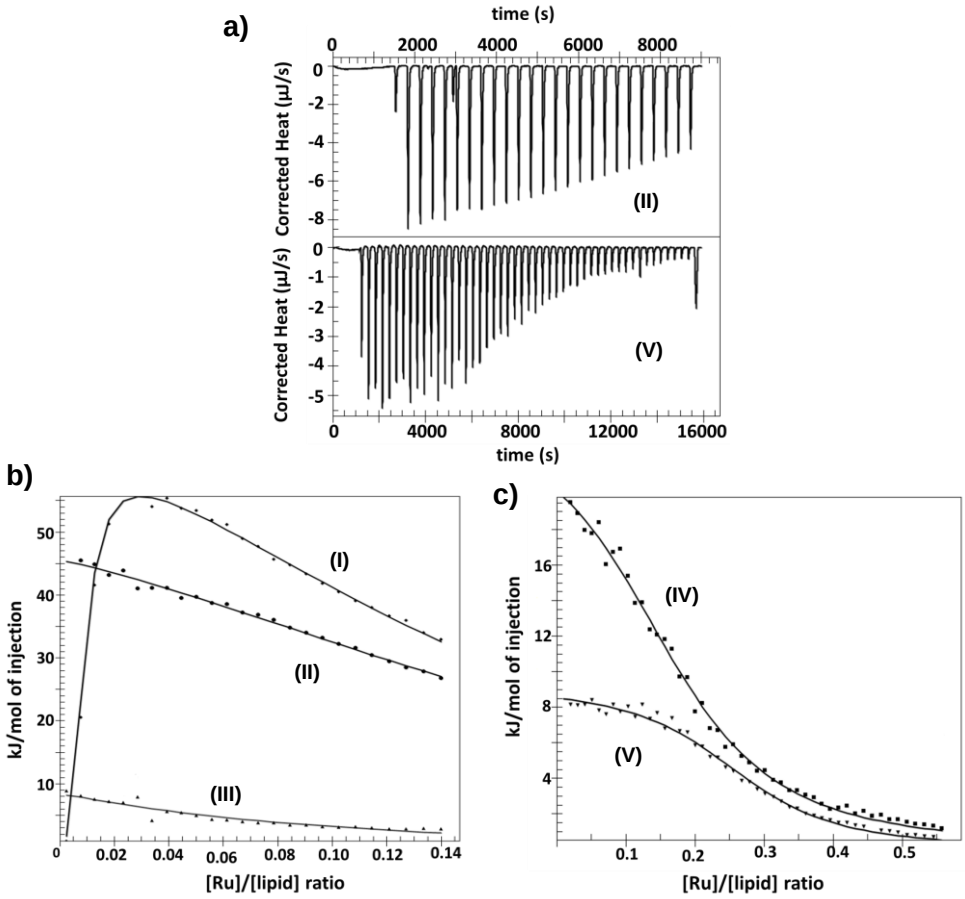

Figure 4.4. Representative binding isotherms obtained upon titration of liposomes with $[\mathbf{2}]^{2+}$ in phosphate buffer at pH=7.0 and 298 K. a) Heat pulses per injection of 10 µL $[\mathbf{2}](PF_6)_2$ (II) or 5 µL of $[\mathbf{2}]Cl_2$ (V) to a liposome solution containing DMPG and 25 mol% ligand **1**. b) and c) corresponding integrated areas (points) and best fitted isotherms; x axis shows the molar ratio between total added ruthenium concentration *[Ru]* and the total lipid concentration *[lipid]* in the solution. Conditions: (I) DMPG and 25 mol% cholesterol (*[lipid]*=1.3 mM, concentration of $[\mathbf{2}](PF_6)_2$ in titrating solution:0.62 mM, *I*=50 mM), (II) DMPG and 25 mol% ligand **1** (*[lipid]*=1.3 mM, concentration of $[\mathbf{2}](PF_6)_2$ in titrating solution:0.62 mM, *I*=50 mM), (III) DMPG and 25 mol% cholesterol (*[lipid]*=1.3 mM, concentration of $[\mathbf{2}](PF_6)_2$ in titrating solution:0.62 mM, *I*=400 mM), (IV) DMPG and 25 mol% cholesterol (*[lipid]*=2.5 mM, concentration of $[\mathbf{2}]Cl_2$ in titrating solution:5 mM, *I*=50 mM), and (V) DMPG and 25 mol% ligand **1** (*[lipid]*=2.5 mM, concentration of $[\mathbf{2}]Cl_2$ in titrating solution:5 mM, *I*=50 mM).

Unlike at lower concentrations the cholesterol-containing DMPG liposomes were found to behave very similarly to DMPG liposomes containing ligand **1**, and only an endothermic adsorption process was observed. Line-fitting of the sigmoidal binding

curves to a single set of *n* identical binding sites provided the adsorption enthalpy ($\Delta H°$), affinity constant (K_a), and binding stoichiometry (*n*), from which the adsorption free energy ($\Delta G°$) and entropy ($\Delta S°$) could be derived (Table 4.1).

For both systems $\Delta H°$ and $\Delta S°$ were found to be positive, while $\Delta G°$ was negative. Thus, the adsorption of the ruthenium complex to the DMPG bilayer is endothermic and driven by entropy. Presumably, the entropy gain upon adsorption is due to the release of water molecules and counter ions (Na^+ ions) when the ruthenium dications come into contact with the phospholipid head groups.[51-55] This interpretation is consistent with monolayer surface pressure experiments, as the surface pressure increased upon adsorption of the complex. Such an increase advocates for the disruption of the hydrogen bonding network between the water molecules and the polar heads of the phospholipids, which must significantly contribute to the overall unfavorable adsorption enthalpy measured by ITC. In addition, comparison between the binding stoichiometry values *n* obtained for the two systems containing cholesterol or ligand **1** revealed that about 5 or 4 lipid molecules, respectively, are bound for each ruthenium complex when saturation of the DMPG liposomes is reached. Since only the outer leaflet of the lipid bilayer is available for adsorption of the ruthenium complex ion, the apparent Ru/lipid ratio at saturation is 2.5 or 2 lipid molecules per ruthenium for cholesterol and ligand **1**, respectively. This stoichiometry almost fits with two monoanionic lipid molecules for one dicationic ruthenium complex, *i.e.*, at saturation of the liposome surface all the initial Na^+ counter cations have been replaced by dicationic ruthenium complexes at the membrane surface. Apparent binding constant values (see Table 4.1) are very close for both systems and rather low, which highlights that sulfur coordination to the ruthenium does not play a significant role at the time scale of these experiments, and that it is mostly the electrostatic adsorption onto the membrane that is actually monitored.

4.3. Discussion

According to our results binding of the ruthenium complex $[\mathbf{2}]^{2+}$ to ligand **1** embedded in a negatively charged liposome occurs *via* a two-step mechanism. As proposed in Scheme 4.1, the outer leaflet of the negatively charged lipid bilayer can be regarded as a "heterogeneous" surface, which first adsorbs ruthenium complexes with fast kinetics (minutes). In a second, slower step (hours), the ruthenium complex $[\mathbf{2}]^{2+}$ undergoes a thermal ligand substitution reaction at the membrane surface, during which the H_2O

ligand is replaced by ligand **1** to form the Ru-S coordination bond ($[\mathbf{3}]^{2+}$). In this model coordination of the sulfur ligand to the metal center occurs *via* two-dimensional diffusion of both the ligand and the metal complex at the membrane surface. Metal binding to ligands embedded in a negatively charged membrane is faster than in homogeneous systems because the fast electrostatic adsorption of the complex to the negative surface of the lipid bilayer increases the local ruthenium concentration near the thioether ligands, *i.e.*, in the electrostatic double layer.[50, 56] Counter-intuitively, the initial adsorption step is not enthalpy driven, because the energy gained by the approach of the dicationic ruthenium center to the negatively charged bilayer must be paid back by removing two monocationic sodium ions. As a result, the adsorption is driven by entropy and occurs *via* dehydration of the phosphate head groups and of the ruthenium dications, and re solvation of the Na^+ monocations. With neutral lipids, *i.e.*, in the absence of electrostatic interaction, hydrophobic interactions are very weak and adsorption does not proceed. Thus, the ruthenium concentration in the electrical double layer, where most of the sulfur ligands are concentrated, remains low, which hampers the coordination reaction.

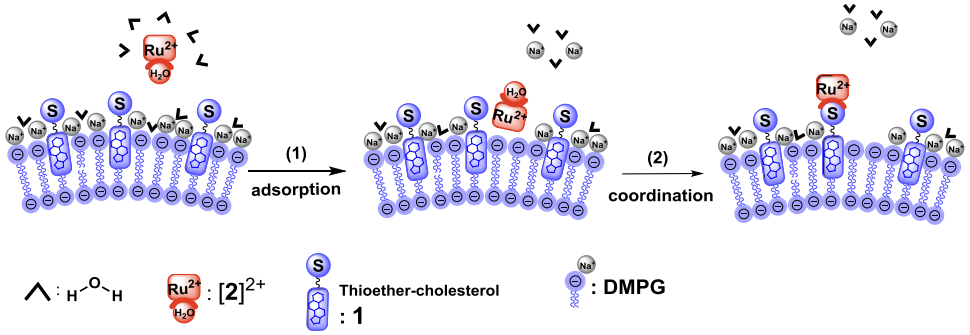

Scheme 4.1. A two-steps model for the thermal binding of the metal complex $[\mathbf{2}]^{2+}$ to ligand **1** embedded in a negatively charged membrane. Step (1): adsorption; step (2): ligand substitution at the water-membrane interface.

Although the charge of metal cations is an important parameter for their adsorption to lipid bilayers, other parameters such as the type of metal cation, the ligands that may be coordinated to it, the number of coordination sites available, and also the surrounding environment (ionic force, pH, *etc.*), all can have a strong influence on the adsorption process. The metal-phospholipid interaction differs from case to case, even when similar divalent cations like Ca^{2+} and Mg^{2+} are used with the same phospholipid.[23-24,

[57-60] Furthermore, upon changing the nature of the lipids the adsorption driving force for a given metal cation may change as well. In a study by Blume *et al.* [61] large negative enthalpies were obtained upon addition of $CaCl_2$ to DMPG liposomes, which was interpreted as a phase transition occurring in the membrane upon adsorption of Ca^{2+}.[53] This interpretation may be relevant to our observations when very low concentrations in $[\mathbf{2}]^{2+}$ (~0.03 mM) come into contact with DMPG liposomes containing cholesterol (1.3 mM, Figure 4.4-I). In contrast, Dimova *et al.*[50] reported the endothermic adsorption of Ca^{2+} ions to mixed neutral/negative liposomes, which is similar to the behavior of higher concentrations in $[\mathbf{2}]^{2+}$ adsorbing on DMPG membranes. Finally, membrane fusion or aggregation does not occur upon addition of $[\mathbf{2}]^{2+}$ to DOPC, DOPG, DMPG, or DMPC membranes, whereas it is a common phenomenon in presence of Ca^{2+} or other divalent cations.[62-63] In spite of their identical charge Ca^{2+} and the Ru(II) complex $[\mathbf{2}]^{2+}$ are quite different, as the latter is surrounded with large, hydrophobic polypyridyl ligands, and has only one potentially available coordination site. Overall, the interaction between metal complex ions and phospholipid membranes appears to comprise a delicate balance between electrostatics, hydrophobic forces, and coordination. In the case of $[\mathbf{2}]^{2+}$ and ligand **1** neither phase changes, nor vesicle aggregation take place, but simply the fast, entropy-driven adsorption of the cation at the water-membrane interface.

4.4. Conclusion

Using three different techniques, the present study distinguishes for the first time the time scales for the adsorption of a dicationic coordination compound on a negatively charged membrane, and the coordination of a membrane-embedded sulfur ligand to the metal center. These results have two major consequences. First, a sequential, two-step model is proposed for the binding of the metal complex to the membrane-embedded ligands. The outer leaflet of a negatively charged lipid bilayer is a surface which quickly adsorbs positively charged metal complexes such as $[\mathbf{2}]^{2+}$. Any slower coordination event will thus take place subsequently, *via* diffusion of both reagents in the two dimensions of the membrane. The relevance of this model for late transition metallodrugs binding to membrane proteins will need to be evaluated.

Secondly, when studying the interaction of metallodrugs with large, negatively charged biomolecules such as DNA, proteins, or lipid membranes, electrostatic interaction may be strong enough to keep the metal complexes in close proximity to the biomolecules

even in absence of coordination to the metal center, which may take place at much longer time scales. In other words, studying the interactions between metal complexes and biomolecules by precipitation or centrifugation experiments, *i e.*, by experimental methods involving short time scales, may conclude to metal-ligand "binding", whereas, formation of the coordination bond between the metal center and the biological ligand did, actually, not occur. This fact should be taken into consideration in future studies looking at the fate of metallodrugs in a biomimetic or biological environment.

4.5. Experimental Section

4.5.1. General

The thioether-cholesterol ligand **1** and the aqua ruthenium complex [**2**]$(PF_6)_2$ were synthesized as reported in Chapter 2. 2-Dimyristoyl-*sn*-glycero-3-phosphoglycerol Sodium salt (DMPG), 1,2-dimyristoyl-*sn*-glycero-3-phosphocholine (DMPC), 1,2-dioleoyl-*sn*-glycero-3-phosphocholine (DOPC), and 1,2-dioleoyl-*sn*-glycero-3-phospho-(1'-rac-glycerol) sodium salt (DOPG) were obtained from Avanti Polar Lipids or Lipoid and stored at −20 °C. Cholesterol, K_2HPO_4, K_2HPO_4, and K_2SO_4 were obtained from commercial sources and used as received. A Perkin-Elmer Lambda 900 UV-vis spectrometer equipped with stirring and temperature control was used for UV-vis measurements. Liposomes size distributions were determined by dynamic light scattering in a Zetasizer (Malvern Instruments Ltd.,U.K.), operated at a wavelength of 633 nm. A KSV Instrument equipped with a 230 mL or 60 mL trough was used for Langmuir monolayer measurements. A NanoITC-2G instrument (TA Instruments, Delaware, USA) with a 1 mL titration cell was used to perform ITC experiments.

4.5.2. Phosphate buffer preparation

Phosphate buffers at pH=7.0 with ionic strengths of 20, 50, 100, 150, 200, 400, 600, 800, and 1000 mM were prepared by dissolving phosphate salts of KH_2PO_4 and K_2HPO_4 (total phosphate salt: 0.90 mmol) and 0.0, 0.97, 2.6, 4.6, 5.9, 12.5, 19.2, 26.0, or 32.5 mmol of K_2SO_4 , respectively, in 100 mL Milli-Q water at 298 K.

4.5.3. Liposome preparation

The lipid (5.0 μmol) and ligand **1** or cholesterol (1.25 μmol) were mixed from chloroform (DOPC, DOPG) or chloroform/methanol 4:1 (DMPG) stock solutions, and dried under reduced pressure using rotary evaporation. The lipid films were subsequently placed under vacuum for at least 1 h to remove traces of organic solvents, and then hydrated in a

phosphate buffer with a desired ionic strength at pH 7.0. The final concentration of the lipids was 2.5 mM. The lipid suspensions were freeze-thawed 10 times above the transition temperature of the corresponding lipid (from liquid N_2 temperature to 323 K), and then extruded 11 times above the transition temperature of the lipid by using an Avanti mini-extruder and polycarbonate membranes with 200 nm pore diameter. The size distribution of the liposomes was measured by DLS to give a value centered between 130 and 150 nm. The samples were kept at 277 K and used within 10 days.

4.5.4. UV-vis measurements

A liposome sample (1.6 mL) containing DMPG, DOPG, or DOPC (2.5 mM) and ligand **1** (25 mol%, 0.62 mM) in a buffer solution (ionic strength: 20, 50, 100, 150, 200, 400, 600, 800, or 1000 mM, pH=7.0), or a solution of Hmte in a buffer with *I*=50 mM (Hmte concentration: 0.62 mM) was placed into a UV-vis cell. 1 mL of the corresponding buffer solution was added to the cuvette and at *t*=0 the volume of the cell was completed by adding $[\mathbf{2}]^{2+}$ in MilliQ (0.4 mL, 0.5 mM stock solution; ratio $[\mathbf{2}]^{2+}$/ligand **1=** 0.5). The final concentrations of the lipid, sulfur ligand, and $[\mathbf{2}]^{2+}$ in the cell were 1.3 mM and 0.3 mM, and 0.067 mM, respectively. The initial absorbance of the sample at 496 nm after base-line correction (subtraction of the absorbance of a liposome sample containing 25 mol% ligand **1** and without ruthenium) was typically 0.46. The sample was stirred in the dark overnight while UV-vis spectra were measured every 3 min, until the thermal equilibrium was reached. The final absorption maximum at 473 nm indicates the formation of complex $[\mathbf{3}]^{2+}$. The plot of $\ln((A_0-A_{inf})/(A_t-A_{inf}))$ *vs.* time was obtained (A_0=Absorbance at *t*=0, A_t=Absorbance at time t, and A_{inf}= absorbance at equilibrium time "t_{inf}", all absorbance values measured at λ=500 nm), and the slope of the plot corresponded to the rate constant (*k*). The half reaction time for each reaction was obtained using the equation $t_{1/2}=\ln(2)/k$.

4.5.5. Langmuir monolayer

All the measurements were performed at pH=7.0 and 298 K. The Teflon troughs and platinum Wilhelmy plate were cleaned properly using cleaning instructions prior to use. Hamilton syringes (25 µL, 50 µL, or 100 µL) were used for monolayer spreading and ruthenium injections.

4.5.6. Surface Pressure-Mean Molecular Area Compression Isotherms

Compression isotherms were carried out on a KSV (U.K.) Langmuir teflon trough (area 24300 mm^2, volume 230 mL). The pure lipid or lipid-ligand spreading solutions were prepared by mixing appropriate volumes of chloroform or chloroform/methanol (4:1) stock

solutions of phospholipids (1 mg/mL) and of ligand **1** or cholesterol (1 mg/mL). Monolayers were formed by depositing small drops of the spreading solutions on the phosphate buffer subphase (pH=7.0, *T*=298 K) with a 25 µL Hamilton microsyringe. For a maximum molecular area of 180 $Å^2$/molecule, around 15 µL of each lipid solution was spread onto the buffer subphase. The monolayers of the desired composition were compressed with 2.4 mm/min and the surface pressure was recorded using a platinum Wilhelmy plate.

4.5.7. Injection of $[2]^{2+}$ and surface pressure *vs.* time isotherms

The experiments were performed on a KSV (U.K.) Langmuir teflon round trough (area 1963 mm^2, volume 65 mL). The pure lipid or lipid-ligand spreading solutions were prepared by mixing appropriate volumes of chloroform or chloroform/methanol (4:1) stock solutions of phospholipids (0.3 mg/mL) and of ligand **1** or cholesterol (0.30 mg/mL). The desired surface pressure for the monolayer corresponded to a specific molecular area ($Å^2$/molecule) as shown in Figure AIV.1. Thus, the amount of lipid spreading solution was estimated for a desired molecular area ($Å^2$/molecule). The monolayers were spread onto the proper subphase (around 8-18 µL of the lipid solution, 3.6 to 8.0 nmol) while recording the surface pressure until a desired surface pressure was obtained. After 20-30 min equilibration, a stock solution of the ruthenium complex [**2**]$(PF_6)_2$ (0.65 mM) (Figure 4.3a) or [**2**]Cl_2 (3.5 mM) (Figures 4.3b and AIV.4) in the appropriate buffer was injected into the subphase and gently mixed (≤100 rpm) at a slow speed taking care not to disturb the monolayer. The surface pressure changes were then recorded until the equilibrium was obtained. Control experiments were performed by injection of [**2**]Cl_2 or [**2**]$(PF_6)_2$ to the subphase without any monolayer or buffer injection under monolayer which did not show any changes on the surface pressure of the subphase.

4.5.8. Isothermal Titration Calorimetry

The experiments were performed on a TA instruments nano-ITC 2G at 298 K and all the solutions were degassed prior to use. The reaction cell (V=1 mL) was filled with the liposome solution containing cholesterol or ligand **1** in the appropriate buffer, and the reference cell with the corresponding liposome-free buffer solution. The liposome solution was titrated by consecutive injections of 5 µL (49 injections) or 10 µL (24 injections preceded by one 5 µl injection) injections of the ruthenium complex $[\mathbf{2}]^{2+}$ solution under constant stirring at 300 rpm. The time interval between successive injections was 300 s. The dilution heat of the ruthenium complexes were determined by injection of $[\mathbf{2}]^{2+}$ into the corresponding buffer and subtracted from the corresponding titrations. Titrations were

duplicated to check reproducibility. The data were analyzed using the NanoAnalyze software TA Instruments, Delaware, USA) using a 1:n independent binding sites model.

4.5.9. Supporting Information available

Surface pressure-mean molecular area compression isotherms (Figure AIV.1); a plot of surface pressure variation upon titration of DMPG monolayers containing 25 mol% ligand **1** with $[\mathbf{2}]^{2+}$ (Figure AIV.2); the surface pressure variation upon injection of $[\mathbf{2}]^{2+}$ to zwitterionic monolayers of DOPC and DMPC (Figure AIV.3); the surface pressure variation upon injection of $[\mathbf{2}]^{2+}$ to DMPG at different Π_0 (Figure AIV.4);ITC and surface pressure data for $[\mathbf{2}](PF_6)_2$ and $[\mathbf{2}]Cl_2$ (Figure AIV.5 and Table AIV.1), are shown as Supplementary Information.

4.6. References

[1] A.-L. Laine, C. Passirani, *Curr. Opin. Pharmacol.* **2012**, *12*, 420-426.
[2] P. J. Stone, A. D. Kelman, F. M. Sinex, *Nature* **1974**, *251*, 736-737.
[3] O. Novakova, J. Kasparkova, O. Vrana, P. M. Vanvliet, J. Reedijk, V. Brabec, *Biochemistry* **1995**, *34*, 12369-12378.
[4] A. P. Martins, A. Marrone, A. Ciancetta, A. Galan Cobo, M. Echevarria, T. F. Moura, N. Re, A. Casini, G. Soveral, *PLoS One* **2012**, *7*, e37435.
[5] C. Metcalfe, J. A. Thomas, *Chem. Soc. Rev.* **2003**, *32*, 215-224.
[6] M. T. Dimanche-Boitrel, O. Meurette, A. Rebillard, S. Lacour, *Drug Resist. Updat.* **2005**, *8*, 5-14.
[7] M. Jensen, M. Bjerring, N. C. Nielsen, W. Nerdal, *J. Biol. Inorg. Chem.* **2010**, *15*, 213-223.
[8] X. Liang, D. J. Campopiano, P. J. Sadler, *Chem. Soc. Rev.* **2007**, *36*, 968-992.
[9] A. Casini, J. Reedijk, *Chem. Sci.* **2012**, *3*, 3135-3144.
[10] G. Mangiapia, G. D'Errico, L. Simeone, C. Irace, A. Radulescu, A. Di Pascale, A. Colonna, D. Montesarchio, L. Paduano, *Biomaterials* **2012**, *33*, 3770-3782.
[11] L. Paasonen, T. Sipila, A. Subrizi, P. Laurinmaki, S. J. Butcher, M. Rappolt, A. Yaghmur, A. Urtti, M. Yliperttula, *J. Control. Release* **2010**, *147*, 136-143.
[12] H. Chen, R. C. MacDonald, S. Li, N. L. Krett, S. T. Rosen, T. V. O'Halloran, *J. Am. Chem. Soc.* **2006**, *128*, 13348-13349.
[13] A. Lau, A. McLaughlin, S. McLaughlin, *Biochim. Biophys. Acta* **1981**, *645*, 279-292.
[14] M. Fragata, F. Bellemare, E. K. Nenonene, *J. Phys. Chem. B* **1997**, *101*, 1916-1921.
[15] W. Hubner, A. Blume, *Chem. Phys. Lipids* **1998**, *96*, 99-123.
[16] M. Suwalsky, B. Ungerer, L. Quevedo, F. Aguilar, C. P. Sotomayor, *J. Inorg. Biochem.* **1998**, *70*, 233-238.
[17] M. J. Scott, M. N. Jones, *Colloids Surf., A* **2001**, *182*, 247-256.
[18] H. Binder, O. Zschornig, *Chem. Phys. Lipids* **2002**, *115*, 39-61.
[19] M. S. Villaverde, S. V. Verstraeten, *Arch. Biochem. Biophys.* **2003**, *417*, 235-243.
[20] S. D. Shoemaker, T. K. Vanderlick, *J. Colloid Interface Sci.* **2003**, *266*, 314-321.

[21] V. Cael, A. Van der Heyden, D. Champmartin, W. Barzyk, P. Rubini, E. Rogalska, *Langmuir* **2003**, *19*, 8697-8708.
[22] P. T. Vernier, M. J. Ziegler, R. Dimova, *Langmuir* **2009**, *25*, 1020-1027.
[23] S. Kewalramani, H. Hlaing, B. M. Ocko, I. Kuzmenko, M. Fukuto, *J. Phys. Chem. Lett.* **2010**, *1*, 489-495.
[24] Y.-H. Wang, A. Collins, L. Guo, K. B. Smith-Dupont, F. Gai, T. Svitkina, P. A. Janmey, *J. Am. Chem. Soc.* **2012**, *134*, 3387-3395.
[25] G. Laroche, E. J. Dufourc, J. Dufourcq, M. Pezolet, *Biochemistry* **1991**, *30*, 3105-3114.
[26] A. P. Ramos, C. Pavani, Y. Iamamoto, M. E. D. Zaniquelli, *J. Colloid Interface Sci.* **2010**, *350*, 148-154.
[27] C. Gasbarri, G. Angelini, A. Fontana, P. De Maria, G. Siani, I. Giannicchi, A. D. Cort, *Biochim. Biophys. Acta, Biomembr.* **2012**, *1818*, 747-752.
[28] G. Speelmans, W. Sips, R. J. H. Grisel, R. Staffhorst, A. M. J. FichtingerSchepman, J. Reedijk, B. deKruijff, *Biochim. Biophys. Acta, Biomembr.* **1996**, *1283*, 60-66.
[29] G. Speelmans, R. Staffhorst, K. Versluis, J. Reedijk, B. deKruijff, *Biochemistry* **1997**, *36*, 10545-10550.
[30] H. Binder, K. Arnold, A. S. Ulrich, O. Zschornig, *Biophys. Chem.* **2001**, *90*, 57-74.
[31] M. Delnomdedieu, A. Boudou, D. Georgescauld, E. J. Dufourc, *Chem-Biol. Interact.* **1992**, *81*, 243-269.
[32] N. S. Raja, K. Sankaranarayanan, A. Dhathathreyan, B. U. Nair, *Biochim. Biophys. Acta, Biomembr.* **2011**, *1808*, 332-340.
[33] D. Voelker, P. Smejtek, *Biophys. J.* **1996**, *70*, 818-830.
[34] S. Bonnet, B. Limburg, J. D. Meeldijk, R. J. M. K. Gebbink, J. A. Killian, *J. Am. Chem. Soc.* **2011**, *133*, 252-261.
[35] D. Marsh, *Biochim. Biophys. Acta* **1996**, *1286*, 183-223.
[36] F. Castelli, M. G. Sarpietro, F. Rocco, M. Ceruti, L. Cattel, *J. Colloid Interface Sci.* **2007**, *313*, 363-368.
[37] O. Maniti, M. Cheniour, O. Marcillat, C. Vial, T. Granjon, *Mol. Membr. Biol.* **2009**, *26*, 171-185.
[38] S. Nathoo, J. K. Litzenberger, D. C. Bay, R. J. Turner, E. J. Prenner, *Chem. Phys. Lipids* **2013**, *167–168*, 33-42.
[39] F. Nsimba Zakanda, L. Lins, K. Nott, M. Paquot, G. Mvumbi Lelo, M. Deleu, *Langmuir* **2012**, *28*, 3524-3533.
[40] E. Polverini, S. Arisi, P. Cavatorta, T. Berzina, L. Cristofolini, A. Fasano, P. Riccio, M. P. Fontana, *Langmuir* **2003**, *19*, 872-877.
[41] F. N. Zakanda, K. Nott, M. Paquot, G. M. Lelo, M. Deleu, *Colloids Surf., B* **2011**, *86*, 176-180.
[42] F. Bringezu, M. Majerowicz, E. Maltseva, S. Y. Wen, G. Brezesinski, A. J. Waring, *ChemBioChem* **2007**, *8*, 1038-1047.
[43] N. Vernoux, O. Maniti, F. Besson, T. Granjon, O. Marcillat, C. Vial, *J. Colloid Interface Sci.* **2007**, *310*, 436-445.
[44] A. Rosengarth, A. Wintergalen, H. J. Galla, H. J. Hinz, V. Gerke, *FEBS Lett.* **1998**, *438*, 279-284.
[45] M. Jesus Sanchez-Martin, I. Haro, M. Asuncion Alsina, M. Antonia Busquets, M. Pujol, *J. Phys. Chem. B* **2010**, *114*, 448-456.
[46] A. Junghans, C. Champagne, P. Cayot, C. Loupiac, I. Koeper, *Langmuir* **2010**, *26*, 12049-12053.
[47] V. Shapovalov, A. Tronin, *Langmuir* **1997**, *13*, 4870-4876.
[48] F. Gambinossi, B. Mecheri, M. Nocentini, M. Puggelli, G. Caminati, *Biophys. Chem.* **2004**, *110*, 101-117.

[49] B. Gzyl-Malcher, M. Filek, G. Brezesinski, *Langmuir* **2011**, *27*, 10886-10893.
[50] C. G. Sinn, M. Antonietti, R. Dimova, *Colloids Surf., A* **2006**, *282*, 410-419.
[51] B. Klasczyk, V. Knecht, R. Lipowsky, R. Dimova, *Langmuir* **2010**, *26*, 18951-18958.
[52] G. J. Gabriel, J. G. Pool, A. Som, J. M. Dabkowski, E. B. Coughlin, M. Muthukurnar, G. N. Tew, *Langmuir* **2008**, *24*, 12489-12495.
[53] R. Lehrmann, J. Seelig, *Biochim. Biophys. Acta, Biomembr.* **1994**, *1189*, 89-95.
[54] M. S. Lin, H. M. Chiu, F. J. Fan, H. T. Tsai, S. S. S. Wang, Y. Chang, W. Y. Chen, *Colloids Surf., B* **2007**, *58*, 231-236.
[55] A. Beck, X. Li-Blatter, A. Seelig, J. Seelig, *J. Phys. Chem. B* **2010**, *114*, 15862-15871.
[56] C. G. Sinn, R. Dimova, M. Antonietti, *Macromolecules* **2004**, *37*, 3444-3450.
[57] N. Duzgunes, J. Wilschut, R. Fraley, D. Papahadjopoulos, *Biochim. Biophys. Acta* **1981**, *642*, 182-195.
[58] A. Martin-Molina, C. Rodriguez-Beas, J. Faraudo, *Biophys. J.* **2012**, *102*, 2095-2103.
[59] J. M. Ruso, L. Besada, P. Martinez-Landeira, L. Seoane, G. Prieto, M. Sarmiento, *J. Liposome Res.* **2003**, *13*, 131-145.
[60] P. Garidel, A. Blume, W. Hubner, *Biochim. Biophys. Acta, Biomembr.* **2000**, *1466*, 245-259.
[61] P. Garidel, A. Blume, *Langmuir* **1999**, *15*, 5526-5534.
[62] D. E. Leckband, C. A. Helm, J. Israelachvili, *Biochemistry* **1993**, *32*, 1127-1140.
[63] D. K. Hincha, *Biochim. Biophys. Acta, Biomembr.* **2003**, *1611*, 180-186.